

Electronic Supplementary Information (ESI) for Dalton Transactions

Structure and spectroscopy of hydrated neptunyl(VI) nitrate complexes

Patric Lindqvist-Reis,*^a Christos Apostolidis,^b Olaf Walter,^{b,c} Remi Marsac,^a Nidhu Lal Banik,^a Mikhail Yu. Skripkin,^d Jörg Rothe^a, Alfred Morgenstern^b

^a Institute for Nuclear Waste Disposal, Karlsruhe Institute of Technology, P.O. Box 3640, 76021 Karlsruhe (Germany)

^b European Commission, Joint Research Centre, Institute for Transuranium Elements P.O. Box 2340, 76125 Karlsruhe (Germany)

^c Institute of Catalysis Research and Technology, Karlsruhe Institute of Technology, P.O. Box 3640, 76021 Karlsruhe, Germany

^d Department of Chemistry, St. Petersburg State University, Universitetsky pr., 26, 198904 St. Petersburg (Russia)

Content:

1. Sample preparation
2. Crystallography
3. EXAFS
4. Vibrational spectroscopy
5. Vis-NIR spectroscopy

1. Sample preparation

$^{237}\text{NpO}_2$ (ca. 170 mg) was dissolved 1 ml concentrated (14 M) HNO_3 by refluxing. The clear solution was then let to boil gently and the excess acid to slowly evaporate until nearly dryness. This slurry was then diluted with 0.5 ml concentrated HNO_3 and heated under reflux for several hours. The dark-red solution was slowly cooled to room temperature, upon which large, dark-red crystals of $[\text{NpO}_2(\text{NO}_3)_2(\text{H}_2\text{O})_2]\cdot\text{H}_2\text{O}$ (**1**) formed (see Fig. S1). The mother liquid (**1aq**) was found to be about 1.2 M with respect to Np and nearly 100% Np(VI) using vis-NIR absorption spectroscopy. Aliquots of **1aq** was used to produce two diluted Np(VI) solutions, 7.9 and 1.6 mM, both of which to be investigated at different concentrations of HNO_3 between 0 and 14 M using vis-NIR absorption spectroscopy (see below).

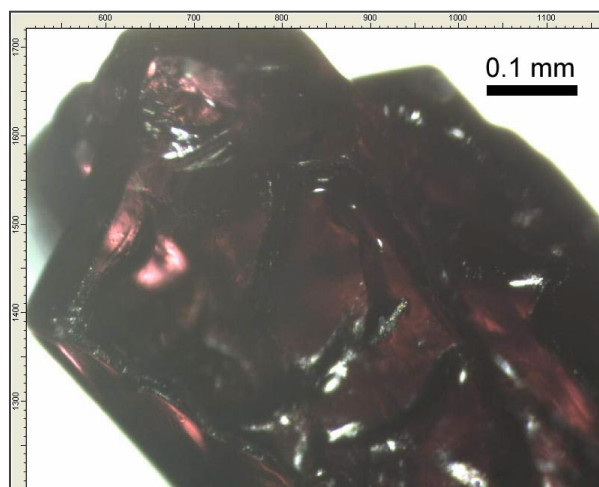


Fig. S1. Light-microscope picture of the dark-red crystals of $[\text{NpO}_2(\text{NO}_3)_2(\text{H}_2\text{O})_2]\cdot\text{H}_2\text{O}$ (**1**).

2. Crystallography

Bruker Apex II Quazar diffractometer. Four spheres of data were collected with an irradiation time of 2 sec per frame at 173 K. The data was corrected for Lorentz and polarization effects and an empirical absorption correction was applied using SADABS.¹ The structure was solved by direct methods with SHELXS, following by additional analysis using difference Fourier maps, and full-matrix least-squares refinement against F^2 using SHELXL, programs of which are contained in a new release of the SHELX-2013 program suit.² All non-hydrogen atoms were refined anisotropically, while all the hydrogen atoms, which could be located from the residual electron density map, were refined isotropically. The thermal ellipsoid plot of **1** depicted in Fig. 1 was prepared with the program Diamond.³ The crystal data, structure refinement and relevant structural data are given in Tables S1-S5. Further details of the crystal structure investigation may be obtained from Fachinformationszentrum Karlsruhe, 76344 Eggenstein-Leopoldshafen, Germany (fax: (+49)7247-808-666; e-mail: crysdata@fiz-karlsruhe.de, http://www.fiz-karlsruhe.de/request_for_deposited_data.html) on quoting CSD 426318.

Table S1 Crystal data and structure refinement for $[\text{NpO}_2(\text{NO}_3)_2(\text{H}_2\text{O})_2] \cdot \text{H}_2\text{O}$ (**1**)

Empirical formula	$\text{H}_6 \text{N}_2 \text{Np O}_{11}$
Formula weight	447.07
Temperature	173(2) K
Wavelength	0.71073 Å
Crystal system	Triclinic
Space group	<i>P</i> -1
Unit cell dimensions	$a = 7.0076(6)$ Å $b = 7.0747(6)$ Å $c = 9.9225(8)$ Å $\alpha = 82.3280(10)^\circ$ $\beta = 82.0830(10)^\circ$ $\gamma = 64.4870(10)^\circ$
Volume	438.21(6) Å ³
Z	2
Density (calculated)	3.388 Mg/m ³
Absorption coefficient	11.912 mm ⁻¹
$F(000)$	402
Crystal size	0.272 × 0.213 × 0.145 mm ³
Theta range for data collection	2.079 to 29.582°
Index ranges	-9≤=h≤=9, -9≤=k≤=9, -13≤=l≤=13
Reflections collected	10954
Independent reflections	2464 [$R(\text{int}) = 0.0441$]
Completeness to theta = 25.242°	99.8 %
Refinement method	Full-matrix least-squares on F^2
Data / restraints / parameters	2464 / 0 / 155
Goodness-of-fit on F^2	1.191
Final R indices [$I > 2\sigma(I)$]	$R_1^a = 0.0266$, $wR_2^b = 0.0719$
R indices (all data)	$R_1^a = 0.0286$, $wR_2^b = 0.0751$
Extinction coefficient	0.204(5)
Largest diff. peak and hole	2.128 and -3.927 e.Å ⁻³

^a $R_1 = \sum |F_o| - |F_c| / \sum |F_o|$. ^b $R_2 = \{\sum w[F_o^2 - F_c^2]^2 / \sum [w(F_o^2)]^2\}^{1/2}$.

Table S2. Atomic coordinates ($\times 10^4$) and equivalent isotropic displacement parameters ($\text{\AA}^2 \times 10^3$) for **1**. $U(\text{eq})$ is defined as one third of the trace of the orthogonalized U^{ij} tensor

	<i>x</i>	<i>y</i>	<i>z</i>	<i>U</i> (eq)
Np(1)	5000	5000	5000	8(1)
Np(2)	5000	0	10000	10(1)
N(1)	1740(3)	8843(3)	6106(2)	15(1)
N(2)	2575(4)	-2332(4)	9542(3)	18(1)
O(1)	4012(3)	5893(3)	3404(2)	18(1)
O(2)	3498(3)	8800(3)	5537(2)	18(1)
O(3)	366(5)	10398(4)	6596(4)	24(1)
O(4)	1497(3)	7171(3)	6121(2)	20(1)
O(5)	2595(7)	3309(7)	5610(5)	22(1)
O(6)	3119(3)	2237(3)	9193(2)	23(1)
O(7)	2343(8)	-1534(8)	10657(4)	21(1)
O(8)	1507(4)	-3207(4)	9328(2)	28(1)
O(9)	3989(3)	-2121(4)	8664(2)	26(1)
O(10)	2915(3)	1001(3)	12172(2)	20(1)
O(11)	9330(4)	4716(4)	7679(3)	19(1)

Table 3. Bond lengths [\AA] and angles [$^\circ$] for **1**

Np(1)-O(1)	1.7450(19)	O(1)-Np(1)-O(4)#1	89.74(8)
Np(1)-O(1)#1	1.7450(19)	O(1)#1-Np(1)-O(4)#1	90.26(8)
Np(1)-O(5)#1	2.429(4)	O(5)#1-Np(1)-O(4)#1	64.20(11)
Np(1)-O(5)	2.429(4)	O(5)-Np(1)-O(4)#1	115.80(11)
Np(1)-O(4)#1	2.4651(18)	O(1)-Np(1)-O(4)	90.26(8)
Np(1)-O(4)	2.4651(18)	O(1)#1-Np(1)-O(4)	89.74(8)
Np(1)-O(2)	2.5319(18)	O(5)#1-Np(1)-O(4)	115.80(11)
Np(1)-O(2)#1	2.5319(18)	O(5)-Np(1)-O(4)	64.20(11)
Np(1)-N(1)#1	2.928(2)	O(4)#1-Np(1)-O(4)	180.0
Np(1)-N(1)	2.928(2)	O(1)-Np(1)-O(2)	88.06(8)
Np(2)-O(6)#2	1.7433(19)	O(1)#1-Np(1)-O(2)	91.94(8)
Np(2)-O(6)	1.7433(19)	O(5)#1-Np(1)-O(2)	64.91(11)
Np(2)-O(10)#2	2.435(2)	O(5)-Np(1)-O(2)	115.09(11)
Np(2)-O(10)	2.435(2)	O(4)#1-Np(1)-O(2)	129.07(6)
Np(2)-O(9)#2	2.493(2)	O(4)-Np(1)-O(2)	50.93(6)
Np(2)-O(9)	2.493(2)	O(1)-Np(1)-O(2)#1	91.94(8)
Np(2)-O(7)#2	2.507(4)	O(1)#1-Np(1)-O(2)#1	88.06(8)
Np(2)-O(7)	2.507(4)	O(5)#1-Np(1)-O(2)#1	115.09(11)
Np(2)-N(2)	2.940(2)	O(5)-Np(1)-O(2)#1	64.91(11)
Np(2)-N(2)#2	2.940(2)	O(4)#1-Np(1)-O(2)#1	50.93(6)
N(1)-O(3)	1.214(3)	O(4)-Np(1)-O(2)#1	129.07(6)
N(1)-O(4)	1.264(3)	O(2)-Np(1)-O(2)#1	180.0
N(1)-O(2)	1.272(3)	O(1)-Np(1)-N(1)#1	90.44(8)
N(2)-O(8)	1.211(3)	O(1)#1-Np(1)-N(1)#1	89.56(8)
N(2)-O(7)	1.268(5)	O(5)#1-Np(1)-N(1)#1	89.48(11)
N(2)-O(9)	1.272(3)	O(5)-Np(1)-N(1)#1	90.52(11)
O(5)-H(5A)	0.74(5)	O(4)#1-Np(1)-N(1)#1	25.29(6)
O(5)-H(5B)	0.76(6)	O(4)-Np(1)-N(1)#1	154.71(6)
O(10)-H(10A)	1.00(6)	O(2)-Np(1)-N(1)#1	154.35(6)
O(10)-H(10B)	0.80(5)	O(1)#1-Np(1)-N(1)	90.44(8)
O(11)-H(11A)	0.83(6)	O(5)#1-Np(1)-N(1)	90.52(11)
O(11)-H(11B)	1.07(8)	O(5)-Np(1)-N(1)	89.48(11)
		O(4)#1-Np(1)-N(1)	154.71(6)
O(1)-Np(1)-O(1)#1	180.00(5)	O(4)-Np(1)-N(1)	25.29(6)
O(1)-Np(1)-O(5)#1	89.54(14)	O(2)-Np(1)-N(1)	25.65(6)
O(1)#1-Np(1)-O(5)#1	90.46(14)	O(2)#1-Np(1)-N(1)	154.35(6)
O(1)-Np(1)-O(5)	90.46(14)	N(1)#1-Np(1)-N(1)	180.00(7)
O(1)#1-Np(1)-O(5)	89.54(14)	O(6)#2-Np(2)-O(6)	180.0
O(5)#1-Np(1)-O(5)	180.0	O(6)#2-Np(2)-O(10)#2	89.02(9)

O(6)-Np(2)-O(10)#2	90.98(9)	O(9)-Np(2)-N(2)#2	154.58(6)
O(6)#2-Np(2)-O(10)	90.98(9)	O(7)#2-Np(2)-N(2)#2	25.35(11)
O(6)-Np(2)-O(10)	89.02(9)	O(7)-Np(2)-N(2)#2	154.65(11)
O(10)#2-Np(2)-O(10)	180.00(11)	N(2)-Np(2)-N(2)#2	180.0
O(6)#2-Np(2)-O(9)#2	87.52(9)	O(3)-N(1)-O(4)	121.8(2)
O(6)-Np(2)-O(9)#2	92.48(9)	O(3)-N(1)-O(2)	122.3(2)
O(10)#2-Np(2)-O(9)#2	115.95(7)	O(4)-N(1)-O(2)	115.9(2)
O(10)-Np(2)-O(9)#2	64.05(7)	O(3)-N(1)-Np(1)	177.9(2)
O(6)#2-Np(2)-O(9)	92.48(9)	O(4)-N(1)-Np(1)	56.43(11)
O(6)-Np(2)-O(9)	87.52(9)	O(2)-N(1)-Np(1)	59.51(12)
O(10)#2-Np(2)-O(9)	64.05(7)	O(8)-N(2)-O(7)	122.2(3)
O(10)-Np(2)-O(9)	115.95(7)	O(8)-N(2)-O(9)	122.7(2)
O(9)#2-Np(2)-O(9)	180.0	O(7)-N(2)-O(9)	115.1(3)
O(6)#2-Np(2)-O(7)#2	91.29(14)	O(8)-N(2)-Np(2)	177.0(2)
O(6)-Np(2)-O(7)#2	88.71(14)	O(7)-N(2)-Np(2)	57.9(2)
O(10)#2-Np(2)-O(7)#2	65.45(11)	O(9)-N(2)-Np(2)	57.24(13)
O(10)-Np(2)-O(7)#2	114.55(11)	N(1)-O(2)-Np(1)	94.84(14)
O(9)#2-Np(2)-O(7)#2	50.75(11)	N(1)-O(4)-Np(1)	98.28(14)
O(9)-Np(2)-O(7)#2	129.25(11)	Np(1)-O(5)-H(5A)	122(3)
O(6)#2-Np(2)-O(7)	88.72(14)	Np(1)-O(5)-H(5B)	125(5)
O(6)-Np(2)-O(7)	91.29(14)	H(5A)-O(5)-H(5B)	110(5)
O(10)#2-Np(2)-O(7)	114.55(11)	N(2)-O(7)-Np(2)	96.8(3)
O(10)-Np(2)-O(7)	65.45(11)	N(2)-O(9)-Np(2)	97.35(15)
O(9)#2-Np(2)-O(7)	129.25(11)	O(6)#2-Np(2)-N(2)	91.35(9)
O(9)-Np(2)-O(7)	50.75(11)	O(6)-Np(2)-N(2)	88.65(9)
O(7)#2-Np(2)-O(7)	180.0	Np(2)-O(10)-H(10A)	127(3)
O(1)#1-Np(1)-N(1)	90.44(8)	Np(2)-O(10)-H(10B)	117(3)
O(5)#1-Np(1)-N(1)	90.52(11)	H(10A)-O(10)-H(10B)	107(4)
O(6)#2-Np(2)-N(2)	91.35(9)	H(11A)-O(11)-H(11B)	100(5)
O(6)-Np(2)-N(2)	88.65(9)		
O(10)#2-Np(2)-N(2)	89.40(7)		
O(10)-Np(2)-N(2)	90.60(7)		
O(9)#2-Np(2)-N(2)	154.58(6)		
O(9)-Np(2)-N(2)	25.42(6)		
O(7)#2-Np(2)-N(2)	154.65(11)		
O(7)-Np(2)-N(2)	25.35(11)		
O(6)#2-Np(2)-N(2)#2	88.65(9)		
O(6)-Np(2)-N(2)#2	91.35(9)		
O(10)#2-Np(2)-N(2)#2	90.60(7)		
O(10)-Np(2)-N(2)#2	89.40(7)		
O(9)#2-Np(2)-N(2)#2	25.42(6)		

Symmetry transformations used to generate equivalent atoms:

#1 -x+1,-y+1,-z+1 #2 -x+1,-y, z+2

Table S4. Anisotropic displacement parameters ($\text{\AA}^2 \times 10^3$) for **1**. The anisotropic displacement factor exponent takes the form: $-2\pi^2 [h^2 a^{*2} U^{11} + \dots + 2 h k a^{*} b^{*} U^{12}]$

	U ¹¹	U ²²	U ³³	U ²³	U ¹³	U ¹²
Np(1)	6(1)	9(1)	10(1)	-2(1)	1(1)	-3(1)
Np(2)	6(1)	12(1)	10(1)	-1(1)	0(1)	-3(1)
N(1)	13(1)	17(1)	15(1)	-2(1)	4(1)	-8(1)
N(2)	18(1)	20(1)	18(1)	-2(1)	1(1)	-10(1)
O(1)	17(1)	23(1)	14(1)	-1(1)	-3(1)	-7(1)
O(2)	13(1)	19(1)	23(1)	-5(1)	6(1)	-9(1)
O(3)	17(1)	15(1)	36(2)	-10(1)	11(1)	-4(1)
O(4)	15(1)	16(1)	29(1)	-7(1)	6(1)	-9(1)
O(5)	17(1)	16(1)	34(2)	-10(1)	12(1)	-10(1)
O(6)	16(1)	22(1)	26(1)	3(1)	-4(1)	-4(1)
O(7)	24(2)	31(2)	12(2)	-6(1)	5(1)	-18(2)
O(8)	31(1)	37(1)	30(1)	-7(1)	-1(1)	-25(1)
O(9)	27(1)	42(1)	19(1)	-12(1)	9(1)	-23(1)
O(10)	16(1)	23(1)	21(1)	-6(1)	7(1)	-9(1)

Table S5. Hydrogen coordinates ($\times 10^4$) and isotropic displacement parameters ($\text{\AA}^2 \times 10^3$) for **1**

	x	y	z	U(eq)
H(5A)	2940(70)	2180(70)	5520(40)	34(11)
H(5B)	1610(100)	3700(100)	6120(60)	70(20)
H(10A)	1900(90)	430(90)	12660(50)	71(15)
H(10B)	2410(80)	2210(80)	12300(50)	51(13)
H(11A)	8670(90)	3970(90)	7820(60)	75(18)
H(11B)	9940(120)	4470(120)	8640(80)	80(30)

3. EXAFS

Np L_3 X-ray absorption spectra of the solid $[\text{NpO}_2(\text{NO}_3)_2(\text{H}_2\text{O})_2] \cdot \text{H}_2\text{O}$ (**1**) compound and the concentrated, 1.2 M Np(VI) in 14 M HNO_3 solution (**1aq**) were recorded at the INE-Beamline for actinide research at ANKA.⁴ A set of germanium (422) crystals ($d = 1.152 \text{ \AA}$) was used for monochromatization of the photon beam. Energy calibration was performed with respect to the position of the first inflection point of a Zr foil K -edge absorption spectrum, which was set to 17.998 keV.⁵ The DCM-crystals were detuned to 70%. The incident and transmitted beam intensities were measured by argon-filled ionization chambers at ambient pressure. The fluorescence photons were recorded by a LEGe five pixel solid state fluorescence detector (Canberra). Six and seven scans of the fluorescence data of **1** and **1aq**, respectively, were averaged (unfortunately, the absorption data were of low quality and so did not permit EXAFS analysis. The low quality of the absorption data was most likely caused by slight movements of the X-ray beam during the data acquisition and/or inadequate sample geometry). The calibrated Np L_3 edges and the XANES regions of **1** and **1aq** are shown in FigS2.

EXAFS oscillations were obtained after performing standard procedures for pre-edge subtraction, normalization and spline removal by means of the WinXAS software.⁶ Fits of the distances to the O and N atoms in the first, second, and third atomic shells within the $[\text{NpO}_2(\text{NO}_3)_2(\text{H}_2\text{O})_2]$ complex of **1** and **1aq** were performed in r -space with FEFFIT⁷, using single and multiple scattering (SS and MS) phase shift and back scattering amplitude functions calculated with FEFF8.2.⁸ The input file to FEFF8.2 for **1** and **1aq** was compiled from the crystal structure of **1** to contain the Cartesian coordinates of each atom but hydrogen within a 5 Å radius from the Np center, which covers the $[\text{NpO}_2(\text{NO}_3)_2(\text{H}_2\text{O})_2]$ complex. The k^3 -weighted data were analyzed in the k -range 3.5–13.9 Å^{−1} and in the r -range 1.0–4.0 Å. $S_0^2 = 0.7(1)$ and $\Delta E_0 = 9(2)$ were obtained from **1** and used as fixed parameters for **1aq**. The relatively low value of S_0^2 (S_0^2 is normally found to be in the range 0.9–1.0) might be linked to self-absorption effects of the fluorescence data, although this is not evident from the XANES region. The coordination numbers (N) in **1** were fixed according to the crystal structure. As to **1aq**, the number of oxygen atoms in the equatorial was refined to 5.5 ± 0.5 , suggesting an equal number of five- and six-coordinated complexes in solution, in which the five-coordinated species would have one nitrate ion in monodentate mode and the other in bidentate mode. However, considering the large error, this model is speculative. In addition, a refinement of the number of nitrogen atoms in coordinating nitrate ions ($\text{N}(\text{NO}_3)$) turned out to be relatively ambiguous, too. The error is large, 2 ± 1 . An unambiguous model based on a refinement of the coordination numbers is thus not possible. On the other hand, the refined bond distances in **1aq** are very close to those of **1**, which in turn, are in good agreement with the distance derived from the crystal structure analysis. The EXAFS and the Fourier transforms with the corresponding fit curves are shown in Fig. S3 and the fit parameters are listed in Table S6.

Table S6 Results of EXAFS least-squares r -space model fitting including SS and MS paths of the first, second, and third atomic shells around Np in the $[\text{NpO}_2(\text{NO}_3)_2(\text{H}_2\text{O})_2]$ complex in **1** and **1aq**.^a Also included is the data from ref.9 for a solution of 0.04 M Np(VI) in 14.5 M HNO_3 .

Sample	$E_{k=0}$ (eV)	Shell	Path	N	R (Å)	σ^2 (Å 2)	ΔE_0 (eV)	S_0^2	Res.
1	17611	O_{ax}	SS	2	1.738(5)	0.0015(4)			
		O_{eq}	SS	6	2.479(8)	0.0042(6)			
		$\text{N}(\text{NO}_3)$	SS	2	2.91(5)	0.008(6)	9(2)	0.7(1)	0.033
		O_{ax}	MS	2	3.52(7)	0.003			
		$\text{N-O}_{\text{dist-N}}$	MS	4	4.08(2)	0.004(2)			
1aq	17611	O_{ax}	SS	2	1.727(7)	0.0016(5)			
		O_{eq}	SS	5.5(5)	2.458(9)	0.0035(7)			
		$\text{N}(\text{NO}_3)$	SS	2(1)	2.98(2)	0.003(2)	9	0.7	0.053
		O_{ax}	MS	2	3.50(3)	0.003			
		$\text{N-O}_{\text{dist-N}}$	MS	4	4.08(3)	0.005(3)			
ref 9	17625	O_{ax}	SS	2.0	1.761	0.0019			
		$\text{O}_{\text{eq}}(\text{H}_2\text{O})$	SS	2.4	2.430	0.0046			
		$\text{O}_{\text{eq}}(\text{NO}_3)$	SS	3.9	2.518	0.0038			
		$\text{N}(\text{NO}_3)$	SS	2.0	2.976	0.0052	8.1	0.9	12.2
		O_{ax}	MS	2.0	3.554	0.0027			
		$\text{O}_{\text{dist}}(\text{NO}_3)$	SS	2.0	4.193	0.0026			
		$\text{N-O}_{\text{dist-N}}$	MS	2.0	4.193	0.0013			

^a Parameters: coordination number N , distance r , Deby-Waller factor σ^2 , amplitude reduction factor S_0^2 , and shift of threshold energy ΔE_0 . Estimated standard deviations are given within brackets. Threshold energy at $k = 0$ $E_{k=0}$.

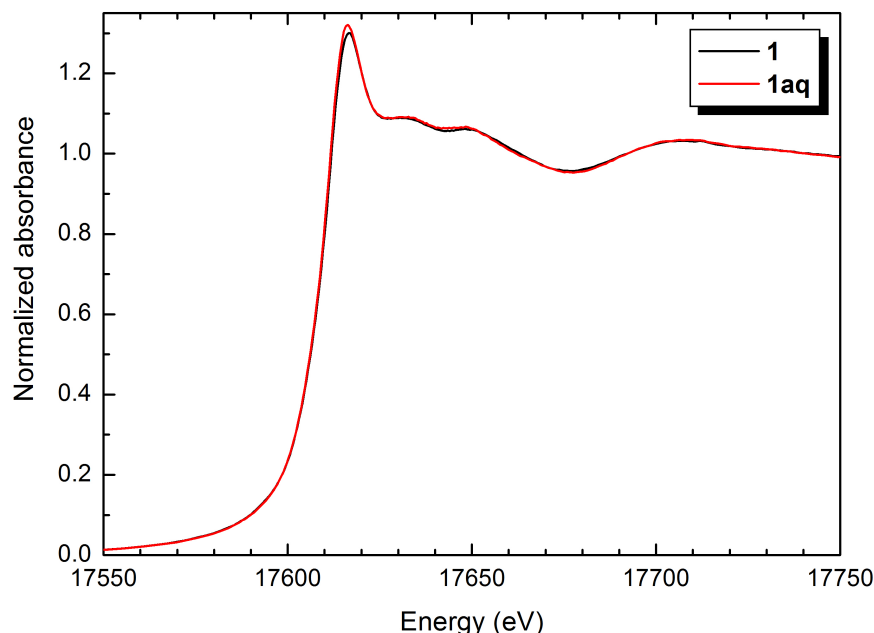


Fig. S2 Np(VI) L_3 edges and the XANES regions of **1** and **1aq**.

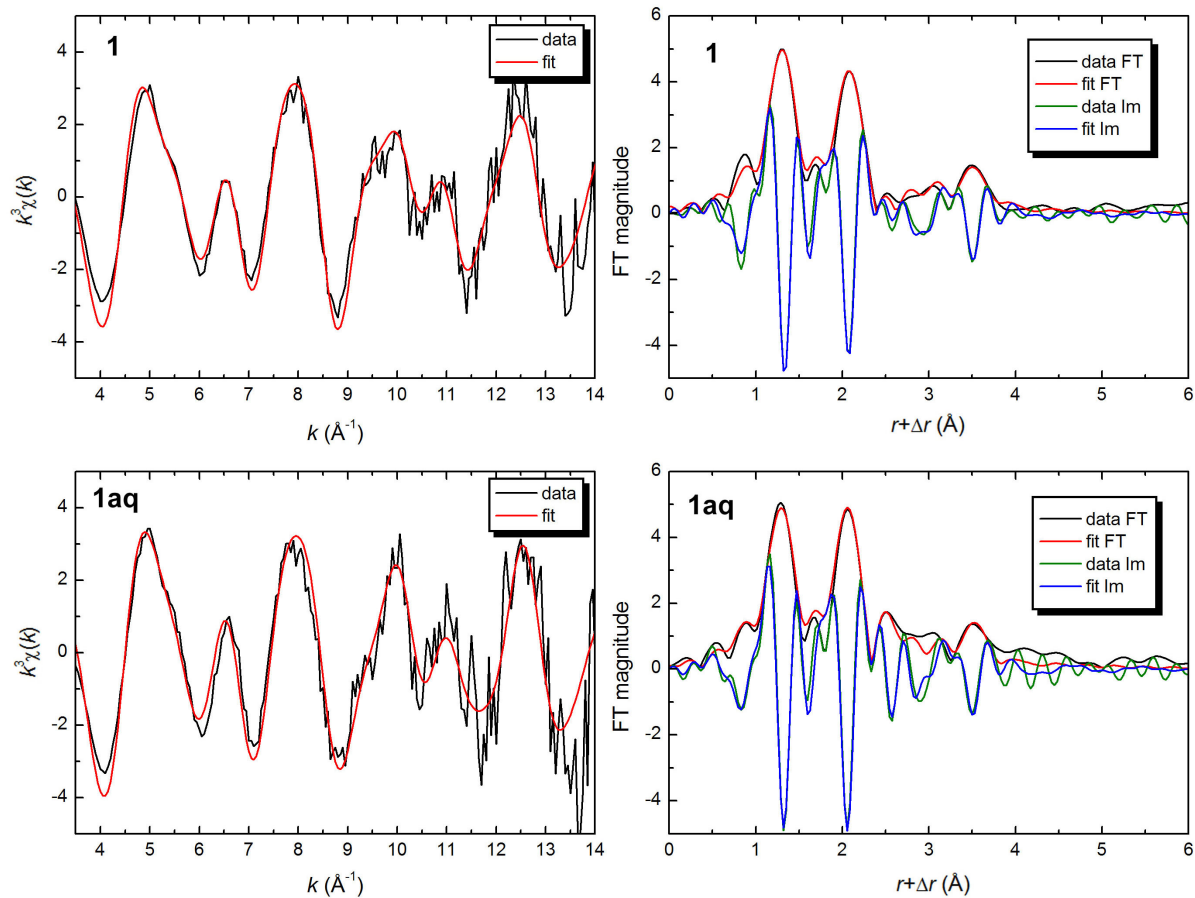


Fig. S3 k^3 -weighted EXAFS data and fitted model functions (left) and the Fourier transforms with fits (right) for **1** and **1aq** (the fitted EXAFS parameters are given in Table S6).

4. Vibrational spectroscopy

Infrared. A Perkin-Elmer Spectrum 400 FTIR-spectrophotometer was used for recording of FIR spectra of **1** and Bruker ALPHA FTIR Platinum ATR for the crystals and the concentrated solution of **1aq** at room temperature. A series of dilutions of **1aq** with water was also undertaken, see Fig. S4. Attempts to measure **1** diluted in KBr tablets in transmission mode showed that this matrix was not inert and resulted in a decomposition of **1**; thus, all measurements, including those of the solutions, were performed using an ATR cell on the “neat” samples.

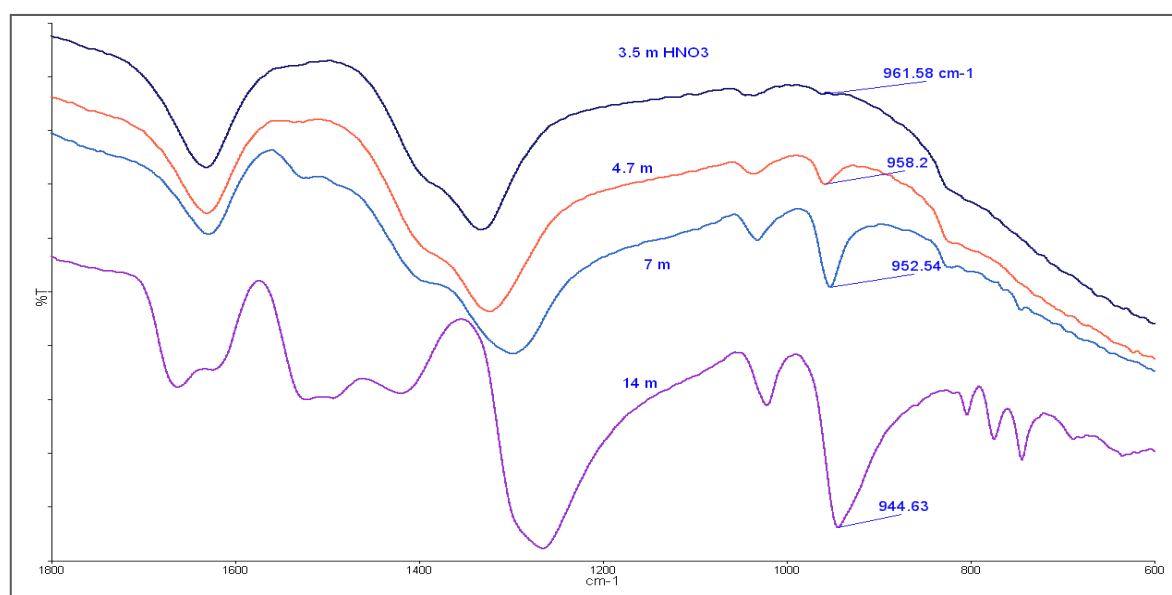


Fig. S4 IR spectra of a series of dilutions with water of the 1.2 M Np(VI) in 14 M HNO₃ (**1aq**) solution, to give solutions containing 7.0, 4.7, and 3.5 M HNO₃. Note the change in frequency of the antisymmetric Np-O vibration from 945 to 962 cm⁻¹ upon dilution with water on going from 14 to 3.5 M nitric acid.

Raman. Raman spectra of **1**, **1aq** and a 14 M HNO₃ aqueous solution were measured at room temperature using a Bruker Senterra dispersive Raman microscope at 532 nm and 10-20 mW at a spectral resolution of 4 cm⁻¹. The radioactive Np samples were contained in screw-capped glass flasks.

5. Vis-NIR spectroscopy

A Perkin-Elmer Lambda 9 UV-Vis-NIR spectrophotometer was used for recording of vis-NIR electronic absorption spectra of **1**, **1aq**, and the dilute (7.9 and 1.6 mM) Np(VI) solutions at different HNO₃ concentrations (0–14 M). The solid sample **1** was diluted in Teflon powder and pressed to a tablet; a quartz cuvette with 1 mm optical path length was used to record the spectrum of **1aq**, while a 10 mm quartz cuvette was used for the two dilute solutions.

Peak deconvolution, and principal component analysis. The NIR absorption spectra of the 7.9 and 1.6 mM Np(VI) solutions at different concentrations of HNO₃ between 0 and 14 M were fitted using the Grams 32 software with a four Gaussian-Lorentzian bands with peak maxima at 1222, 1228, 1220, and 1080 nm, suggesting that there are four different aqueous Np(VI) species in solution, assigned to [NpO₂]²⁺ (1222 nm), [NpO₂(NO₃)]⁺ (1228 nm) and [NpO₂(NO₃)₂] (1120; 1080 nm), as discussed in the article. Fig. S5 shows the four component bands. Note that the component band for the [NpO₂]²⁺(aq) (1222 nm) species is represented by the spectrum at 0 M HNO₃. Also note that the difference in the peak height of the bands is a result of a difference in molar extinction. Because the band at 1080 nm is mainly seen (as a shoulder) at 14 M HNO₃ and has negligible intensity at lower HNO₃ concentrations, three component bands are sufficient to fit all spectra reasonably well. Fig. S6 shows the fitted spectra of the 7.9 mM Np(VI) solution at 8.5 and 14 mM HNO₃.

An independent analysis of the spectra was performed using the ITFA program, which performs principal component analysis, iterative target transformation analysis and varimax rotations.¹⁰ Indeed, using four component bands resulted in a negligible contribution of the 1080 nm band, whereas with only two component bands the ITFA program was unable to account for the slight redshift from 1222 to 1228 nm appearing in the spectra of the solutions up to 10 M HNO₃ (Fig. S7). Final fits were therefore performed with three components. The derived component spectra with the corresponding species distributions are shown for the 7.9 and 1.6 mM Np(VI) solutions in Fig. S8 and Fig. S9, respectively.

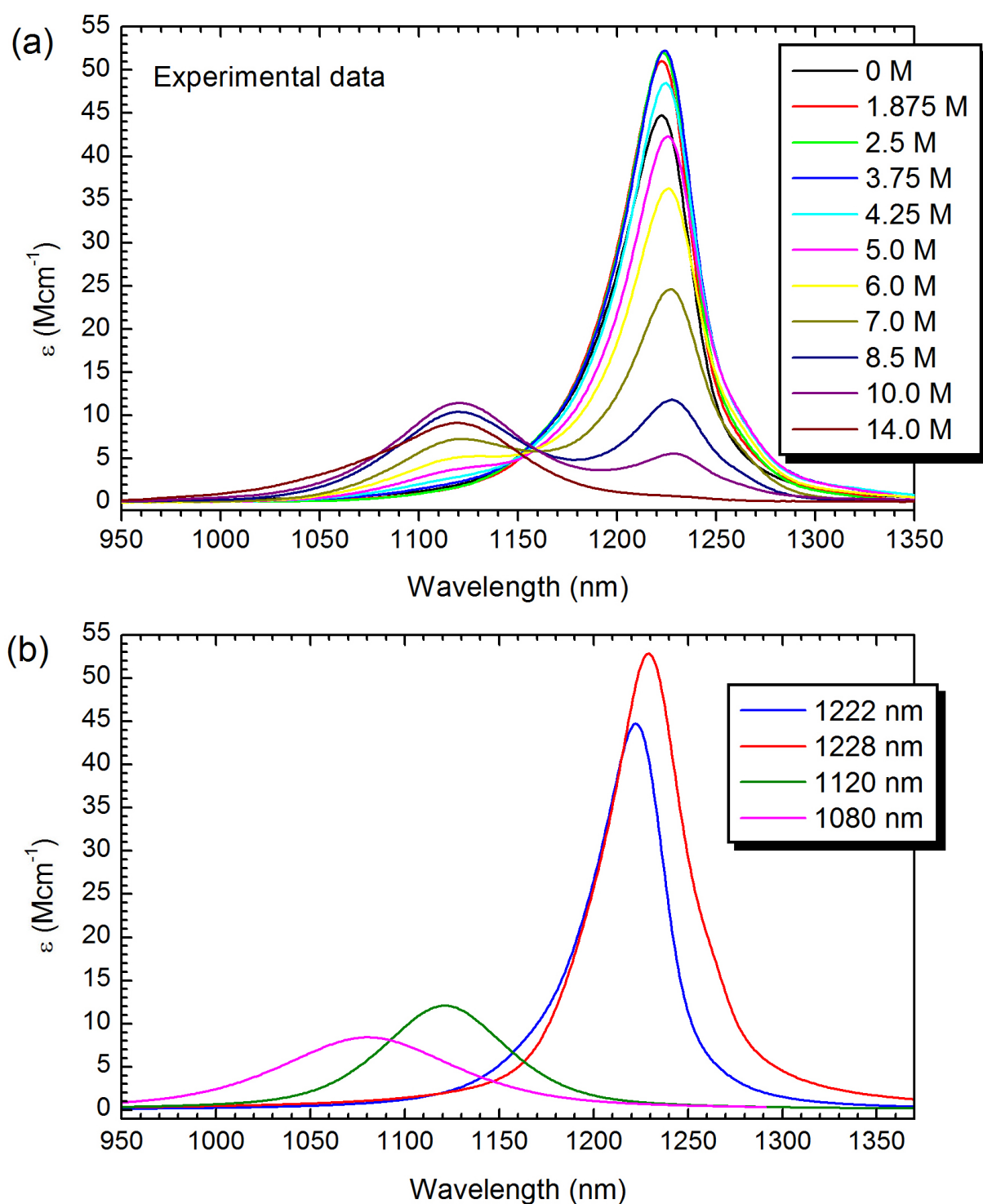


Fig. S5 (a) NIR absorption spectra of the 7.9 mM Np(VI) solutions, converted from absorbance to absorptivity ($M^{-1}cm^{-1}$) units. (b) Pure component spectra obtained by peak deconvolution using three Gaussian-Lorentzian bands (provided in the Grams 32 software) and the spectrum at 0 M NO_3^- as a reference for the pure component spectrum of 100 % $[NpO_2^{2+}]$ (aq). The extinction coefficients at peak maximum of the component four bands are about 45, 53, 12, and 8 $M^{-1}cm^{-1}$ for the $[NpO_2]^{2+}$ ($\lambda_{max} = 1222$ nm), $[NpO_2(NO_3)]^+$ (1228 nm), $[NpO_2(NO_3)_2]$ (1120 nm), and $[NpO_2(NO_3)_2]$ (1080 nm) species, respectively.

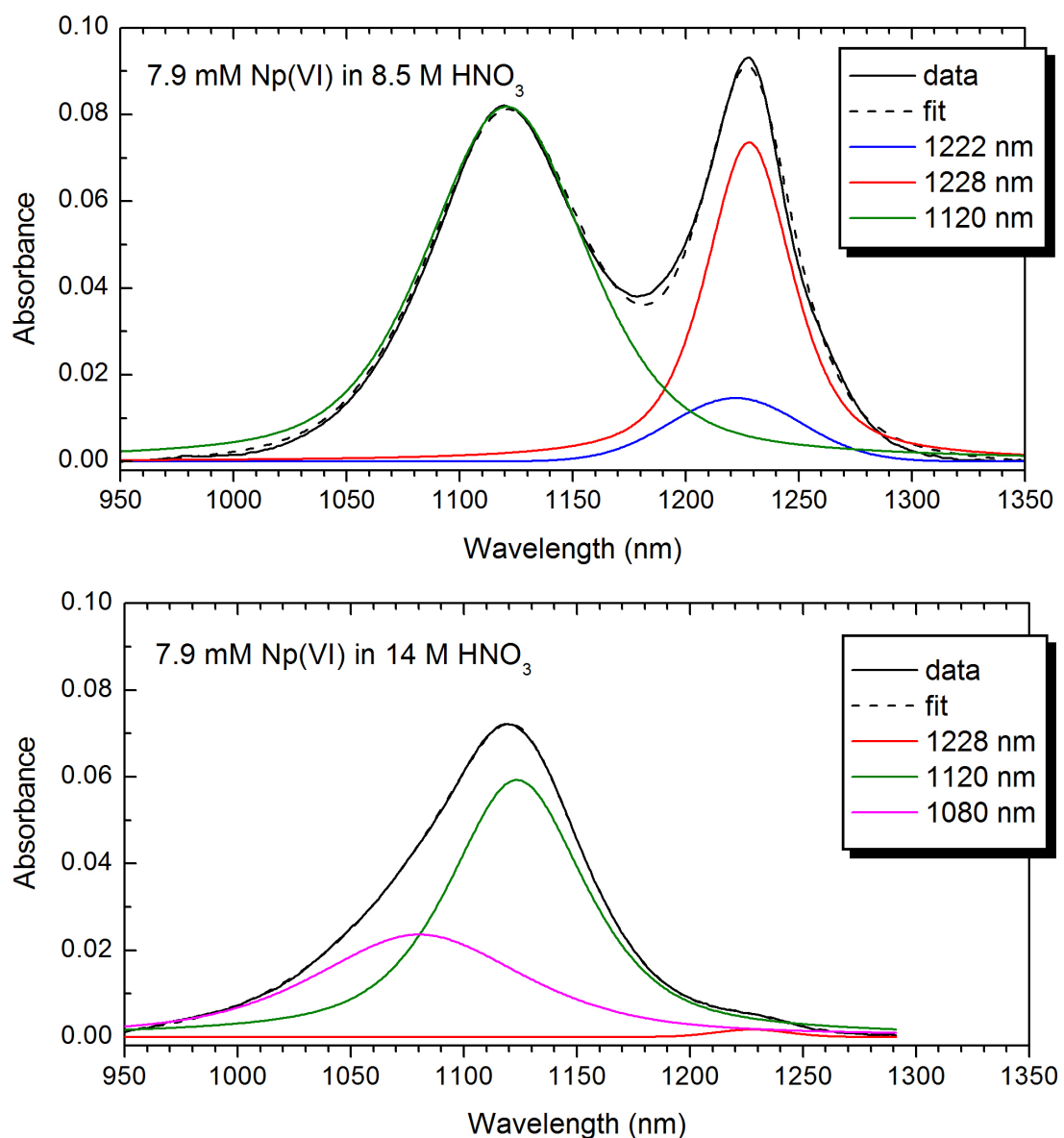


Fig. S6 Peak deconvolution (using Grams 32) of NIR absorption spectra of the 7.9 mM Np(VI) solutions at 8.5 and 14 M HNO_3 .

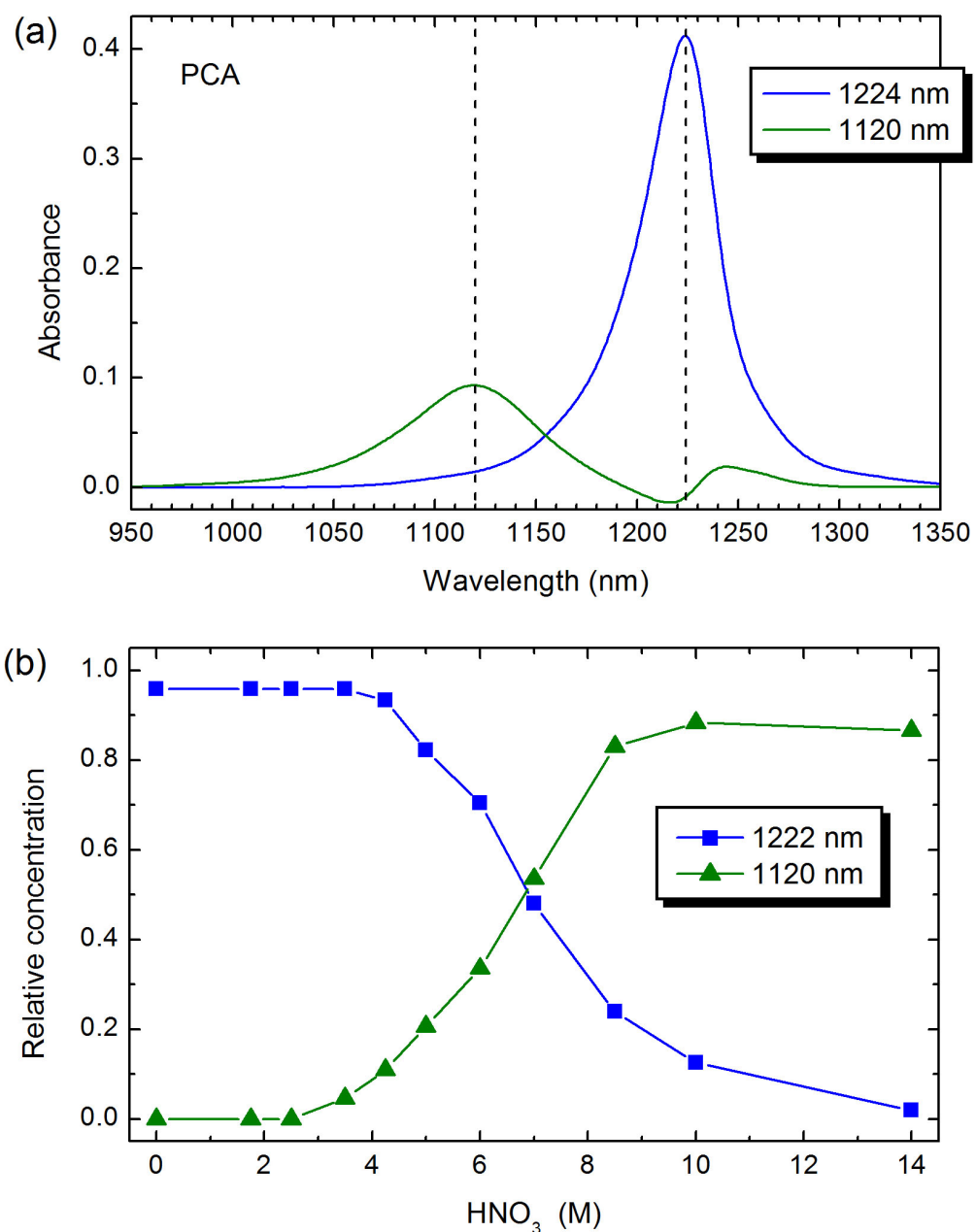


Fig. S7 Principal component analysis performed with two components. (a) Component spectra with peak maxima at 1224 and 1120 nm. Note that the redshift observed from 1222 to 1228 nm in the experimental spectra, which is most likely due to the presence of two different Np(VI) species, is here accounted for by one component band at 1224 nm. Also note that the component band at 1120 nm has a small residual peak near 1245 nm. (b) Distributions of the two different Np(VI) species as a function of HNO_3 concentration.

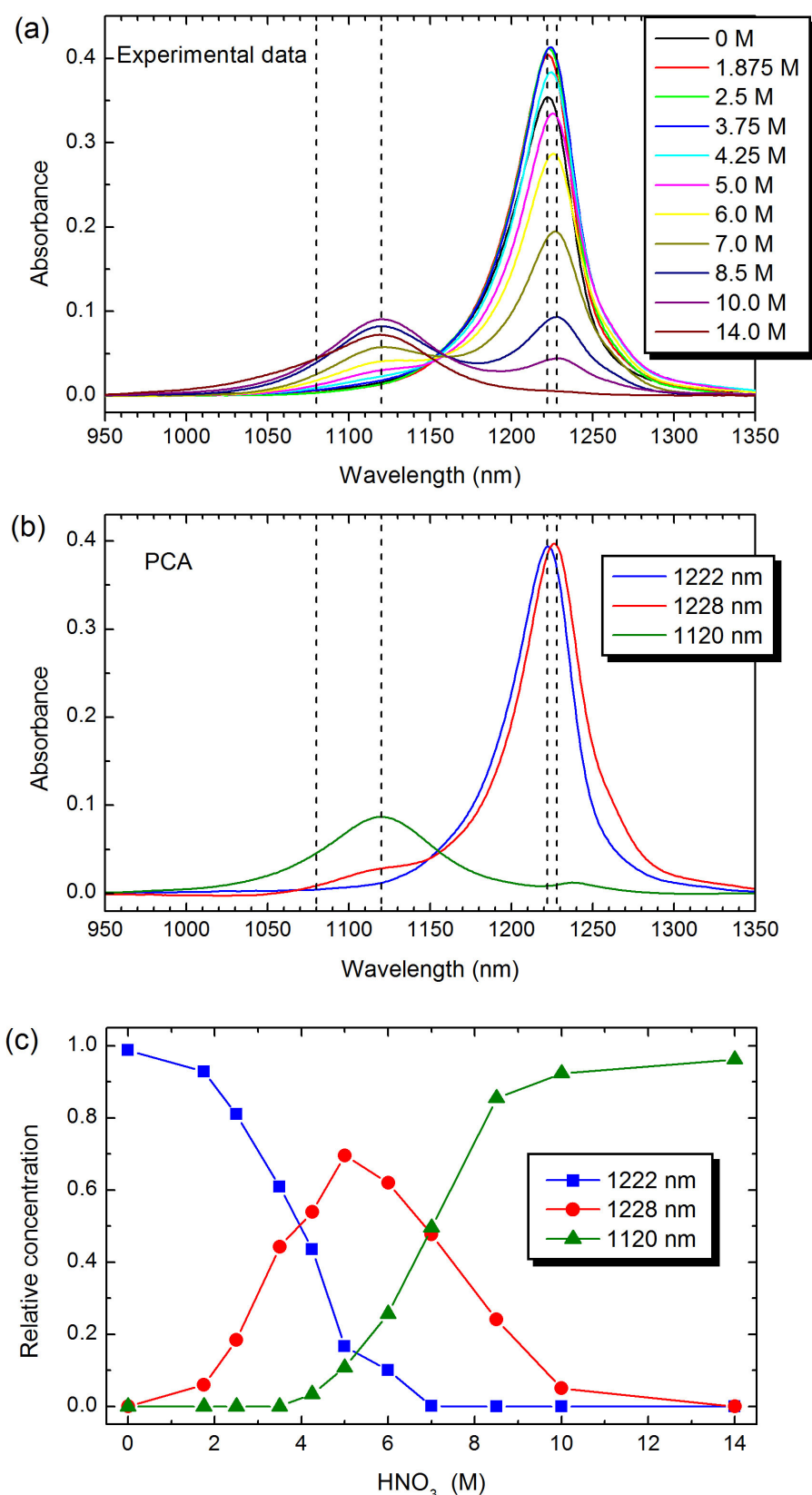


Fig. S8 (a) NIR absorption spectra of 7.9 mM Np(VI) in aqueous solutions at different HNO₃ concentrations ranging from 0 to 14 M (the 0 M solution is represented by a 1 M HCF₃SO₃ solution). (b) The three component bands obtained with the ITFA program. A small residual band is seen at about 1240 nm in the “1120 nm” component band. (c) Distributions of the different Np(VI) species as a function of HNO₃ concentration.

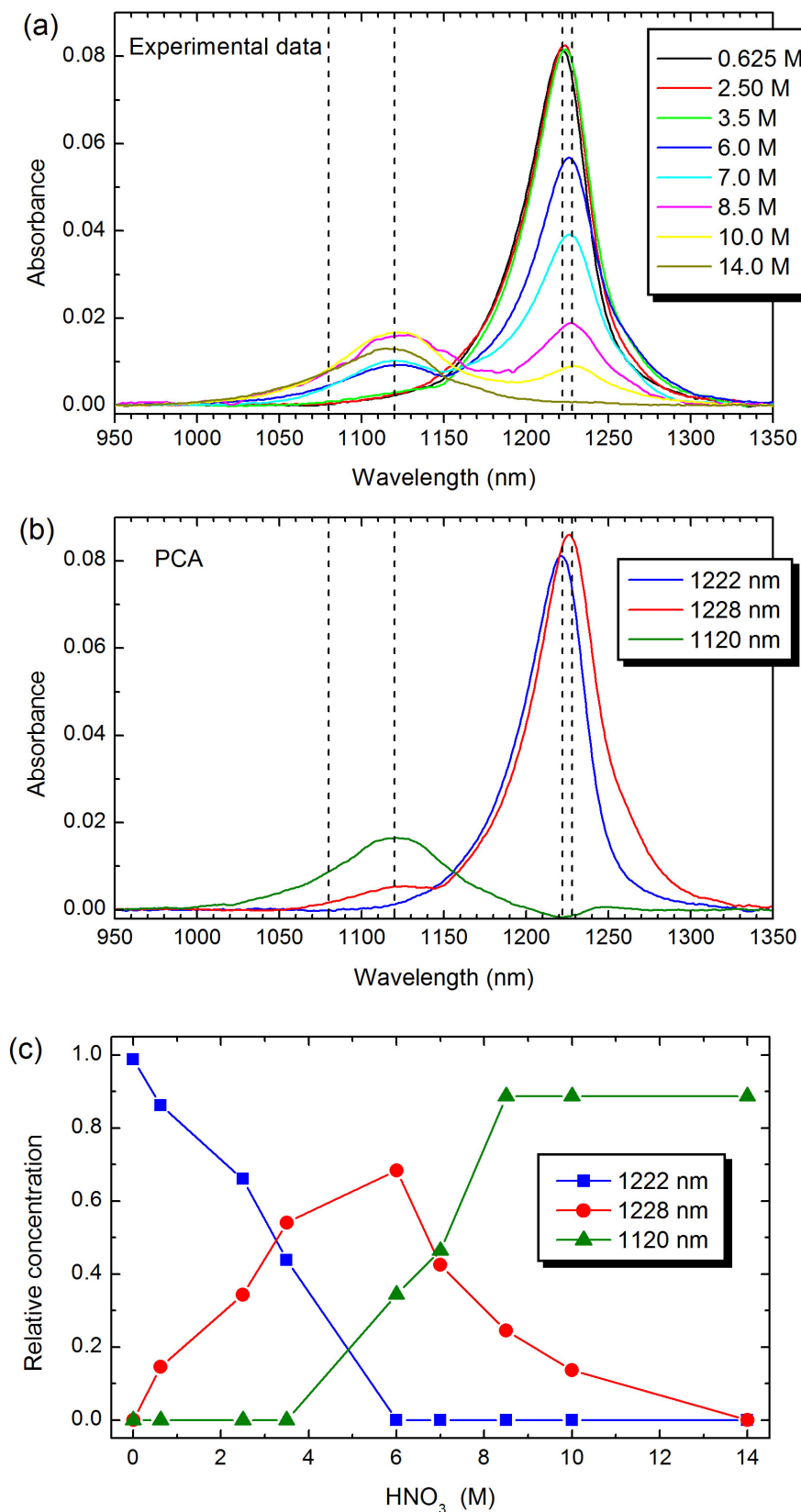


Fig. S9 (a) NIR absorption spectra of 1.6 mM Np(VI) in aqueous solutions at different HNO_3 concentrations up to 14 M. (b) The three component bands obtained with the ITFA program. A small is seen at about 1240 nm in the “1120 nm” component band. (c) Distributions of the different Np(VI) species as a function of HNO_3 concentration.

-
- 1 SADABS, empirical absorption correction, Bruker Analytical X-ray Systems, Madison, WI, 1998.
 - 2 SHELX-2013 is a program suit for crystal structure solution and refinement by G. M. Sheldrick, University of Göttingen, Germany, 2013.
 - 3 DIAMOND-Visual Crystal Structure Information System, CRYSTAL IMPACT, Postfach 1251, D-53002 Bonn, Germany.
 - 4 J. Rothe, S. Butorin, K. Dardenne, M.A. Denecke, B. Kienzler, M. Löble, V. Metz, A. Seibert, M. Steppert, T. Vitova, C. Walther and H. Geckeis, *Rev. Sci. Instrum.* 2012, **83**, 043105.
 - 5 J.A. Bearden and A.F. Burr, *Rev. Mod. Phys.* 1967, **39**, 125.
 - 6 Ressler, T. *J. Synchrotron Radiation*, 1998, **5**, 118.
 - 7 M. Newville, B. Ravel, D. Haskel, J.J. Rehr, E.A. Stern and Y. Yacoby, *Physica B*, 1995, **208**, 209.
 - 8 A.L. Ankudinov, B. Ravel, J.J. Rehr and S.D Conradson, *Phys. Rev. B*, 1998, **58**, 7565.
 - 9 A. Ikeda-Ohno, C. Hennig, A. Rossberg, H. Funke, A. C. Scheinost, G. Bernhard and T. Yaita, *Inorg. Chem.* 2008, **47**, 8294.
 - 10 A. Rossberg, T. Reich and G. Bernhard, *Anal. Bioanal. Chem.*, 2003, **376**, 631.